JAST, Vol. 5, No. 2, pp 67–79

JAST Journal of Aerospace Science and Technology

Development of a Novel Method in TRMC for a Binary Gas Flow Inside a Rotating Cylinder

A. A. Ganjaei[1], S. S. Nourazar[2], Sh. Navardi[3] and S. M. Hosseini[4]

A new approach to calculating the axially symmetric binary gas flow is proposed. Dalton's law for partial pressures contributed to by each species of a binary gas mixture (argon and helium) is incorporated into numerical simulation of rarefied axially symmetric flow inside a rotating cylinder using the time relaxed Monte-Carlo (TRMC) scheme, and the direct simulation Monte-Carlo (DSMC) method. The results of the flow simulations are compared with the analytical solution and those obtained by Bird, (1994). Such results show better agreements than Bird's in comparison with the analytical solutions. However, the results of the flow simulations using the TRMC scheme show better agreement than those obtained using the DSMC method when compared with the analytical solutions.

NOMENCLATURE

f_p	The velocity probability distribution functions of the molecule of the species p having a velocity of v.
f_{1p}	The velocity probability distribution functions of the molecule of the species p having a velocity of v_1.
f^*	The post-collision velocity probability distribution functions of the molecule of the species p having a velocity of v.
f^*_{1p}	The post-collision velocity probability distribution functions of the molecule of the species p having a velocity of v_1.
f	The mass density distribution function.
k	The Boltzmann constant.
M_w	The molecular weight.
$M(v)$	The Maxwellian velocity distribution.
m	Mass of a molecule of gas.
d	Diameter of a molecule of gas.
m_r	Reduced mass.
n	The number density of molecules.
N	The total number of molecules.
r	The radial distance.
R	The cylinder radius.
T	The absolute temperature.
V	Velocity of a class of molecules.
$\bar{v}_0$	The mean macroscopic velocity.
v'	Thermal velocity.
$\bar{v}_i$	The mean velocity of species i.
T_{Tr}	Translation temperature.
v^*	The post collision velocity.
y	The Molar Fraction.
ϵ	The Knudsen number.
μ	The mean collision frequency for molecules having the velocity V.
σ	Collisional cross section of molecules.
ρ	Density of gas.
γ	Temperature exponent of the coefficient viscosity.
ω	The angular velocity.
θ	Planar angle.
Ω	The angle in the spherical coordinates.

1. *PhD Candidate, Dept. of Mech. Eng., Amirkabir Univ. of Tech., Tehran, Iran, Email: aganjaei@aut.ac.ir*
2. *Associate Professor, Dept. of Mech. Eng., Amirkabir Univ. of Tech., Tehran, Iran.*
3. *MSc. Graduate, Dept. of Mech. Eng., Amirkabir Univ. of Tech., Tehran, Iran.*
4. *MSc. Graduate, Dept. of Mech. Eng., Amirkabir Univ. of Tech., Tehran, Iran.*

INTRODUCTION

In the gas flow problems, where the length scale of the system is comparable to the mean free path of molecules in the gas flow, the concept of the continuum is no more valid, with Knudsen number greater than 0.1, Bird, (1994). In this case, the simulation is done using the Direct Simulation Monte-Carlo (DSMC) or the Collisional Boltzmann Equation (CBE) methods, Hockney *et.al.*, (1981) and Nanbu, (1986). In most cases, the direct solution of the CBE is impracticable due to the huge number of molecules; however, most of the time the implementation of the DSMC is more practicable. Thus far, a class of Monte-Carlo method has been used to simulate the rarefied gas dynamic problems. The rarefied hypersonic flow is solved using the DSMC method by Bird, (1994). The comparison between the Navier-Stokes and the DSMC methods for the simulation of the cicumnuclear coma is done by Crifo *et.al.* (2002). The simulation of the rarefied gas flow through circular tube of finite length in the transitional regime at both low Knudsen number and high Knudsen number is done using the DSMC method by Shinagawa *et.al.*, (2002). Recently Bottoni, (2004) used the molecular approach based upon a Monte-Carlo simulation for sodium vapor flow of mono-atomic molecules in liquid metal fast breeder reactor bundle. Simulation of flows like recirculation flow problems or near continuum flows are still expensive due to the particular nature of the DSMC method (Myong, 2004). However, Pareschi *et.al.*, (1999) proposed a modification to the DSMC method to circumvent this problem. Pareschi *et.al.*, (2001) used the time relaxed Monte-Carlo (TRMC) method with the wild sum expansion (Wild, 1951) to approximate the non negative function describing the time evolution of the distribution function of particles. However, the optimal choice of the coefficients in the Wild sum expansion for the distribution function of particles is left as an open problem. Pareschi *et.al.*, (2005) numerically simulated the Boltzmann equation for a two-dimensional gas dynamic flow around an obstacle using the TRMC method. Their simulation showed improvement over the DSMC method in terms of computational efficiency. Nourazar *et.al.*, (2005), compared the simulation of the Navier-Stokes and the Boltzmann equations of the axially symmetric compressible flow past a flat nosed cylinder at high velocity and low pressure with shock wave using the Monte-Carlo method. The results of the two simulations are compared in terms of different Knudsen numbers.

Purpose of the Present Work

In the simulation of rarefied gas dynamic problems, when the Knudsen number is small, collisions occur at a fast rate; therefore, a kinetic treatment (DSMC) of the problem is extremely expensive due to the required small time-step. Since the ratio of time scales between macroscopic and microscopic effects is large enough; therefore, reaching the stationary results of flow characteristics may almost be impossible.

On the other hand, the TRMC schemes allow the use of larger time-steps than those required by the DSMC method; thereby allowing one to achieve the stationary results of flow properties in a comparatively shorter computational time. To our knowledge, no researcher has so far tried to incorporate the new idea of using the Dalton's law in the simulation of axially symmetric binary gas flow when implementing the TRMC scheme. In the present work, we intend to simulate the flow properties of binary gas mixture (argon and helium) inside a rotating cylinder using the TRMC scheme and the DSMC method. The results of the simulations using the two methods are compared with the analytical solutions and those obtained by Bird 1994 for the same case study problem. In the simulation using the DSMC, we follow exactly the same procedures described in Bird 1994, and in the one using the TRMC, we follow exactly the same procedures described in Pareschi *et.al.* 2005.

Description of the Case Study Problem

The cylinder rotates at the tangential velocity of 1000 meter/second and the radius of the cylinder is 1 meter. The gas mixture inside the cylinder comprises of 50% argon and 50% helium; the initial temperature of the gas mixture inside the rotating cylinder is 200 Kelvin and the initial pressure of the gas mixture inside the cylinder is 2.76 Pascal absolute. These data are the same as those presented in Bird 1994.

MATHEMATICAL FORMULATIONS

The Boltzmann Equation

The Boltzmann equation for the temporal evolution of particles velocity distribution function for species p is written as (Bird, 1994):

$$\frac{\partial}{\partial t}\left(n_p f_p\right) + V_p . \frac{\partial}{\partial r}\left(n_p f_p\right) = \frac{1}{\varepsilon}\sum_{q=1}^{s} Q\left(n_p f_p, n_q f_q\right) \cdot \quad (1)$$

In Eq. (1), n is the density of molecules of species, f is the probability distribution function of the molecules of species having velocity V, f_1 is the probability distribution function of the molecules of species having velocity V_1, ϵ is Knudsen number which is equal to the ratio of λ, the mean free path between collisions, to the characteristic length L. The subscripts p and q represent the particular species.

The bilinear collisional operator $Q\left(n_p f_p, n_q f_q\right)$, which describes the binary collisions of the molecules

is given by:

$$Q\left(n_p f_p, n_q f_q\right) = \sum_{q=1}^{s} \int_{-\infty}^{+\infty} \int_{0}^{4\pi} n_p n_q \left[f_p^* f_{1q}^* - f_p f_{1q}\right] \sigma\left(\left|V_{rpq}\right|, \Omega\right) d\Omega\, dV_{1q}. \tag{2}$$

where, $V_{r_{pq}}$ is the relative velocity between the molecules of species p and species q, and Ω is a vector of the unitary sphere. The kernel σ is a non-negative function which is described as (Pareschi, 2005):

$$\sigma\left(\left|V_{rpq}\right|, \Omega\right) = b_\alpha\left(\theta\right)\left|V_{rpq}\right|^\alpha \cdot \tag{3}$$

where, θ is the scattering angle between $V_{r_{pq}}$ and $V_{r_{pq}}\Omega$. The Variable Hard Sphere (VHS) (Bird, 1994) model is often used in the numerical simulation of rarefied gases, where, $b_\alpha(\theta) = \varepsilon C$ with C a positive constant and $\alpha = l$. The value of C is equal to (Bird, 1994), $C = \sigma_{pq}$.

Substituting Eq. (3) into Eq. (2), we get:

$$\frac{1}{\varepsilon} Q\left(n_p f_p, n_q f_q\right) = \sum_{q=1}^{s} \int_{-\infty}^{+\infty} \int_{0}^{4\pi} n_p n_q \sigma_{pq} V_{rpq} \left[f_p^* f_{1q}^* - f_p f_{1q}\right] d\Omega\, dV_{1q}. \tag{4}$$

Substituting the bilinear collisional operator (Eq. (4)) into Eq. (1), the Boltzmann equation is written as:

$$\frac{\partial}{\partial t}\left(n_p f_p\right) + V_p . \frac{\partial}{\partial r}\left(n_p f_p\right) = \frac{1}{\varepsilon} Q\left(n_p f_p, n_q f_q\right) = \sum_{q=1}^{s} \int_{-\infty}^{+\infty} \int_{0}^{4\pi} n_p n_q \sigma_{pq} V_{rpq} \left[f_p^* f_{1q}^* - f_p f_{1q}\right] d\Omega\, dV_{1q}. \tag{5}$$

In Eq. (5), n is the density of molecules of species, f is the probability distribution function of the molecules of species having velocity V, f_1 is the distribution function of the molecules of species having velocity V_1, f^* is the post-collision probability distribution function of the molecules of species having velocity V and f_1^* is the post-collision probability distribution function of the molecules of species having velocity V_1. The subscripts p and q represent the particular species.

The DSMC and TRMC Schemes

In the binary gas mixture flow with two different species p and q, the Boltzmann equation can be separately written for the species in the following manner:

$$\frac{\partial}{\partial t}\left(n_p f_p\right) + V_p . \frac{\partial}{\partial r}\left(n_p f_p\right) = \frac{1}{\varepsilon} Q\left(n_p f_p, n_p f_p\right) + \frac{1}{\varepsilon} Q\left(n_p f_p, n_q f_q\right) \cdot \tag{6}$$

In the present work, the Dalton law is used to calculate the pressure of the mixture, which is calculated as $P = P_p + P_q$, where P_p is the partial pressure of the species p, and P_q is the partial pressure of the species q. The density of the mixture is calculated as $\rho_m = y_{Ar}\rho_{Ar} + y_{He}\rho_{He}$, where ρ_m is the mixture density, y_{Ar} is the molar fraction of argon, ρ_{Ar} is the density of argon, y_{He} is the molar fraction of helium and ρ_{He} is the density of helium. First, we assume that only the argon gas exists inside the rotating cylinder, and the flow is simulated using the TRMC and the DSMC methods. Second, we assume that only the helium gas exists inside the rotating cylinder, and that the flow is simulated using the TRMC and the DSMC methods. In both cases, the effect of collisions of molecules of argon and the effect of collisions of molecules of helium are considered separately, $Q\left(n_p f_p, n_q f_q\right) = 0$.

$$\frac{\partial}{\partial t}\left(n_p f_p\right) + V_p . \frac{\partial}{\partial r}\left(n_p f_p\right) = \frac{1}{\varepsilon} Q\left(n_p f_p, n_p f_p\right) \cdot \tag{7}$$

We split Eq. (7) (Gabetta, *et.al.*, 1997) into equation for the effect of collision, $\frac{\partial}{\partial r}\left(n_p f_p\right) \equiv 0$, and equation for the effect of convection, $Q\left(n_p f_p, n_p f_p\right) = 0$. The equation for the effect of collision is written as (Pareschi, 2005):

$$\frac{\partial}{\partial t}\left(n_p f_p\right) = \frac{1}{\varepsilon} Q\left(n_p f_p, n_p f_p\right) \cdot \tag{8}$$

For simplicity, we omit the index and replace $n_p f_p$ with f, where f is the mass density function of the molecules of species having velocity V. Then Eq. (8) is rewritable as:

$$\frac{\partial}{\partial t}\left(f\right) = \frac{1}{\varepsilon} Q\left(f, f\right), \tag{9}$$

and the collision term is written as:

$$\frac{1}{\varepsilon} Q\left(f, f\right) = \int_{-\infty}^{+\infty} \int_{0}^{4\pi} \sigma V_r \left[f^* f_1^* - f f_1\right] d\Omega\, dV_1 = \int_{-\infty}^{+\infty} \int_{0}^{4\pi} \sigma V_r f^* f_1^* d\Omega\, dV_1 - f \int_{-\infty}^{+\infty} \int_{0}^{4\pi} \sigma V_r f_1 d\Omega\, dV_1 = \frac{1}{\varepsilon}\left[P\left(f, f\right) - \mu\left(V\right) f\right] \cdot \tag{10}$$

where, $\mu\left(V\right) = \int_{-\infty}^{+\infty} \int_{0}^{4\pi} \sigma V_r f_1 d\Omega V_1 = \int_{0}^{4\pi} \sigma V_r d\Omega \int_{-\infty}^{+\infty} f_1 dV_1 = \kappa\rho/m$ is the mean collision frequency for the molecules having velocity V, ρ is the density of the gas, m is the mass of a molecule of the gas, κ is a molecular constant $\kappa = \int_{0}^{4\pi} \sigma V_r\, d\Omega$ and $\rho/m = \int_{-\infty}^{+\infty} f_1\, dV_1$ (Wild, 1951). In

the special case in which σV_r is independent of V_r (Maxwellian molecules), we have:

$$\mu(V) = \mu = \frac{\kappa\rho}{m} \tag{11}$$

Plugging Eqs. 10 and 11 into Eq. 9:

$$\frac{\partial f}{\partial t} = \frac{1}{\varepsilon} Q(f,f) = \frac{1}{\varepsilon}\left[P(f,f) - \mu f\right]\cdot \tag{12}$$

The first order time discretization of Eq. 12 is written as:

$$\frac{f^{n+1} - f^n}{\Delta t} = \frac{1}{\varepsilon}\left[P(f^n, f^n) - \mu f^n\right]$$

$$f^{n+1} = \left(1 - \frac{\mu\,\Delta t}{\varepsilon}\right) f^n + \frac{\mu\,\Delta t}{\varepsilon}\frac{P(f^n, f^n)}{\mu}\cdot \tag{13}$$

The probabilistic interpretation of Eq. 13 is the following. In order for a particle to be sampled from f^{n+1}, a particle is sampled from f^n, with the probability of $(1 - \mu\,\Delta t/\varepsilon)$, and a particle is sampled from $P(f^n, f^n)/\mu$, with the probability of $\mu\,\Delta t/\varepsilon$. It is to be noted that the above probabilistic interpretation fails if the ratio of $\mu\,\Delta t/\varepsilon$ is too large because the coefficient of f^n on the right hand side may become negative. This means that in the stiff region (where the Knudsen number is small $\varepsilon << l$), the time step becomes extremely small; therefore, the method becomes almost unstable near the fluid regime (Nanbu 1980 and Babovsky 1986).

To circumvent the problem, the new independent variable τ and new dependent variable $F(V,\tau)$ is defined as:

$$\tau = \left(1 - e^{-\mu t/\varepsilon}\right) \tag{14}$$

$$F(V,\tau) = f(V,t)\, e^{\mu t/\varepsilon}. \tag{15}$$

Therefore, Eq. (12) is rewritten as:

$$\frac{\partial F}{\partial \tau} = \frac{1}{\mu} P(F,F)$$

$$F(V, \tau = 0) = f(V,0)\cdot \tag{16}$$

Eq. (16) is Cauchy problem, and it has a power series solution such as follows (Gabetta *et.al.* 1997):

$$F(V,\tau) = \sum_{k=0}^{\infty} \tau^k f_k(V)$$

$$f_{k=0}(V) = f(V,0)\cdot \tag{17}$$

Substituting Eq. (17) in Eq. (16), we have:

$$\frac{\partial F}{\partial \tau} = \sum_{k=0}^{\infty} k\tau^{k-1} f_k = \sum_{k=0}^{\infty} (k+1)\,\tau^k f_{k+1}$$

$$P(F,F) = P\left(\sum_{k=0}^{\infty} \tau^k f_k, \sum_{k=0}^{\infty} \tau^k f_k\right)\cdot \tag{18}$$

Expanding the summation terms gives us:

$$\frac{\partial F}{\partial \tau} = f_1 + 2\tau f_2 + 3\tau^2 f_3 + 4\tau^3 f_4 + \cdots$$

$$P(F,F) = P\left(f_0 + \tau f_1 + \tau^2 f_2 + \cdots,\right.$$
$$\left. f_0 + \tau f_1 + \tau^2 f_2 + \cdots\right)\cdot \tag{19}$$

Plugging Eq. (19) into Eq. (16):

$$f_1 + 2\tau f_2 + 3\tau^2 f_3 + 4\tau^3 f_4 + \cdots$$
$$= \frac{1}{\mu} P\left(f_0 + \tau f_1 + \tau^2 f_2 + \cdots, f_0 + \tau f_1 + \tau^2 f_2 + \cdots\right)$$
$$= \frac{1}{\mu}\left[P(f_0,f_0) + \tau P(f_0,f_1) + \tau P(f_1,f_0)\right.$$
$$\left. + \tau^2 P(f_0,f_2) + \tau^2 P(f_2,f_0) + \tau^2 P(f_1,f_1) + \cdots\right]$$
$$= \frac{1}{\mu}\left[P(f_0,f_0) + 2\tau P(f_0,f_1) + 2\tau^2 P(f_0,f_2)\right.$$
$$\left. + \tau^2 P(f_1,f_1) + \cdots\right] = \frac{1}{\mu}\left[P(f_0,f_0) + 2\tau P(f_0,f_1)\right.$$
$$\left. + \tau^2\left\{2P(f_0,f_2) + P(f_1,f_1)\right\} + \cdots\right]\cdot \tag{20}$$

Equating the coefficients of corresponding powers of τ, we can find the value of f to be:

$$f_1 = \frac{1}{\mu} P(f_0,f_0),$$

$$f_2 = \frac{1}{\mu} P(f_0,f_1),$$

$$f_3 = \frac{1}{\mu}\left\{\frac{2}{3} P(f_0,f_2) + \frac{1}{3} P(f_1,f_1)\right\}\cdot$$

$$\vdots \tag{21}$$

Therefore, the function f is found by the recurrence formula to be:

$$f_{k+1} = \frac{1}{k+1}\sum_{h=0}^{k} \frac{1}{\mu} P(f_h, f_{k-h}), \qquad k = 0, 1, \ldots\cdot \tag{22}$$

Converting Eq. (17) into the original variables, we obtain the following formula representing the solution to the Cauchy problem 9:

$$f(v,t) = e^{-\mu t/\varepsilon} \sum_{k=0}^{\infty} \left(1 - e^{-\mu t/\varepsilon}\right)^k f_k(v)\cdot \tag{23}$$

A class of numerical schemes based on a suitable truncation for $m \geq 1$ of Eq. (23) is derived (Gabetta *et.al.*, 1997):

$$f(v,t) = e^{-\mu t/\varepsilon} \sum_{k=0}^{m} \left(1 - e^{-\mu t/\varepsilon}\right)^k f_k(v)$$
$$+ \left(1 - e^{-\mu t/\varepsilon}\right)^{m+1} M(v)\cdot \tag{24}$$

where $f^n = f(n\Delta t)$, and Δt is the time step. The quantity M in Eq. (24) is the asymptotic solution to the equation, and is called Maxwellian.

Eq. (24) can be generalized using different weight functions including the influence of the higher order coefficients. In general, the TRMC scheme is written as:

$$f^{n+1} = \sum_{k=0}^{m} A_k f_k + A_{m+1} M \cdot \tag{25}$$

where, the functions f_k are given by Eq. (22) and the weight functions $A_k(\tau)$ are non-negative functions that satisfy the consistency, conservation and the asymptotic preservation conditions (Gabetta *et.al.* 1997). In this simulation, the first order TRMC of Eq. (25) as $f^{n+1} = A_0 f_0^n + A_1 f_1 + A_2 M$ is used.

ANALYTICAL SOLUTIONS

The energy E of a particle in an axially symmetric gas mixture flow inside a rotating cylinder is given as (Kuo, L. Y., 1990),

$$E(r) = \frac{1}{2} I\omega^2 = \frac{1}{2} m r^2 \omega^2. \tag{26}$$

The rotational effect is the same as that of the additional external field acting on the system, and may be written as:

$$U(r) = -\frac{1}{2} m r^2 \omega^2. \tag{27}$$

Using the Boltzmann distribution for the particle number density and substituting for $U(r)$ from Eq. (27), we have:

$$n(r) = A \exp\left(-\frac{U(r)}{kT}\right) = A \exp\left(\frac{m r^2 \omega^2}{2kT}\right). \tag{28}$$

where the normalization factor A can be determined by $N = \int n(r) dV$ giving:

$$N = \int_0^R \int_0^{2\pi} A \exp\left(-\frac{U(r)}{kT}\right) r dr d\theta$$

$$= \int_0^R \int_0^{2\pi} A \exp\left(\frac{m r^2 \omega^2}{2kT}\right) r dr d\theta, \tag{29}$$

$$N = 2\pi A \int_0^R \exp\left(\frac{m r^2 \omega^2}{2kT}\right) r dr$$

$$= \pi A \int_0^R \exp\left(\frac{m r^2 \omega^2}{2kT}\right) d(r^2) = \pi A \tfrac{2kT}{m\omega^2} \exp\left(\frac{m r^2 \omega^2}{2kT}\right)\Bigg|_0^R$$

$$= \tfrac{2\pi A k T}{m\omega^2}\left(\exp\left(\frac{m R^2 \omega^2}{2kT}\right) - 1\right). \tag{30}$$

Then for A, we can have:

$$A = \tfrac{N m \omega^2}{2\pi k T}\left(\exp\left(\frac{m R^2 \omega^2}{2kT}\right) - 1\right)^{-1}. \tag{31}$$

Therefore:

$$n(r) = \frac{N m \omega^2}{2\pi k T L} \cdot \frac{\exp\left(\frac{m\omega^2 r^2}{2kT}\right)}{\exp\left(\frac{m\omega^2 R^2}{2kT}\right) - 1}. \tag{32}$$

where, N is the total number of molecules, m is the mass of a molecule of gas, ω is the angular velocity, k is the Boltzmann constant, T is the absolute temperature, L is the length of the cylinder, R is the cylinder radius and r is the radial distance.

BOUNDARY AND INITIAL CONDITIONS

Boundary conditions

At the boundary where the axis of symmetry exists, the rule of specular reflection is considered. The specular reflection rule is implemented for molecules at the solid surface boundary with normal velocity to the solid boundary being reversed and those with parallel velocity to the solid surface boundary remaining unchanged. At the top and bottom boundary of the cylinder the rule of specular reflection, and at the wall of the cylinder the rule of diffusion reflection apply. The diffuse reflection rule is implemented for molecules at the solid surface boundary with a velocity component equal to the tangential velocity at the cylinder wall equal to 1000 meter/second, and the other component of the velocity is equal to the most probable velocity according to the Maxwellian equilibrium distribution. Therefore, the resultant velocity is equal to the velocity obtained on the basis of the kinetic theory of gases. In the diffuse reflection rule, the temperature of the reflected molecule and the temperature of the solid wall boundary need to be equal and the velocities of the reflected molecules are distributed according to Maxwellian equilibrium distribution.

Initial conditions

The initial values of the gas mixture pressure and the temperature are 2.76 Pascal absolute and 200 Kelvin respectively. The molar concentrations of the gas mixture inside the cylinder consist of 50% argon and 50% helium. The initial velocities of the molecules are obtained based on the kinetic theory.

THE NUMERICAL PROCEDURES

In the simulation of the problem using the DSMC method, two grid systems are chosen. The first grid system (Figure 1) is used to calculate the averaging of the flow properties. This grid system is chosen to be fine enough in order to increase our computational accuracy. The grid system is refined until the variations

of the flow properties are not substantial (the variations of the flow properties are less than 2%). The second grid system is chosen to be very fine (the mesh size is equal to 0.2 times the mean free path of the molecules); therefore, the collision of the molecules are controlled within each mesh accurately. Our grid system consists of 5 times 100 meshes, and the total number of model molecules is 35700. The number of real molecules is obtained based on the density of gas and the Avogadro's number, where each model molecule consists of $5.49735*10^{15}$ real molecules. In the TRMC scheme, the same grid system (5 times 100) and the same number of model molecules, *i.e.* 35700, are used. The number of real molecules is obtained based on the density of gas and the Avogadro's number. For the axially symmetric flows, the distribution of the modeled molecules is linearly proportional to the radial distance. The volume of the mesh far from the axis of symmetry is much larger than the volume of the mesh close to the axis of symmetry. Therefore, the number of the modeled molecules far from the axis of symmetry is much greater than the number of modeled molecules close to the axis of symmetry. This leads to the uniformity of density in the radial direction. The size of the mesh is in order of the mean free path, and the time step in our simulation is chosen to be 0.2 times the mean collision time of Bird, 1994. The molecules are distributed in the mesh system according to the normal distribution. The initial velocity of the molecules is chosen based on the kinetic theory of gases. The direction of velocity of the molecules is chosen randomly based on the equilibrium Maxwellian distribution. We then start to advance with time, and the new position of the molecules is designated. The collisions of the model molecules are done based on the variable hard sphere (VHS) model proposed by Bird, 1994. We then continue advancing in time until the statistical fluctuations of the flow properties is minimum. In the simulation of gas mixture (argon and helium) flow inside the high speed rotating cylinder, the gas mixture pressure inside the cylinder is initially 2.76 Pascal absolute, the radius of the cylinder is 1 meter, the tangential velocity at the cylinder wall is 1000 meter/second, the gas mixture inside the cylinder consists of 50% argon and 50% helium, and the temperature of the gas mixture inside the cylinder is 200 Kelvin. The total number of 35700 model molecules is considered to be distributed linearly along the radial coordinates.

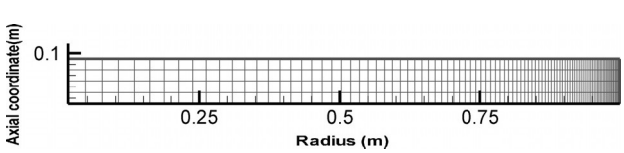

Figure 1. The structure of mesh system for the cylinder of radius 1meter and height of 0.1 meter.

The time-step of the simulation is chosen to be 10^{-6} second and the simulation is done until 25.7 seconds of real time (1280000 iterations) in DSMC method. In the TRMC scheme, the time-step of the simulation is chosen to be $5*10^{-6}$ second and the simulation is done until 25.7 seconds of real time (256000 iterations). The calculations are performed by the IBM compatible personal computer with a 2.8 GHz CPU and a 512 MB RAM.

Algorithm of the Direct Simulation Monte Carlo Method (DSMC)

DSMC Algorithm (for the VHS collision model molecules)

- $T_{ref} = 273$ K
- $d_{p_{ref}} = 2.33 \times 10^{-10}$, for He
- $d_{q_{ref}} = 4.17 \times 10^{-10}$, for Ar
- $m_r = \frac{m_p m_q}{m_p + m_q}$
- $k = 1.380658 \times 10^{-23}$ jK^{-1}
- $\Delta t = 1 \times 10^{-6}$ Sec
- Distribute the initial locations of the particles according to the uniform distribution.
- for $n_t = 1$ to n_{tot}:
  1. Given $\{v_i^n, i = 1, \ldots, N\}$.
  2. Define the local Knudsen number (ε).
  3. Calculate

$$d_{pq} = (d_{ref})_{pq} \left[\left\{2k\left(T_{ref}\right)_{pq} / \left(m_r \left|v_i - v_j\right|^2\right)\right\}^{\gamma_{pq}-1/2} / \Gamma\left(5/2 - \gamma_{pq}\right)\right].$$

  4. Compute an upper bound $\bar{\sigma} = \max\left((\pi/4)\, d_{pq}^2 \left(|v_i - v_j|\right)\right)$ for the cross section, $\bar{\sigma}$ is updated in each collision.
  5. Set $\mu = 4\pi\bar{\sigma}$.
  6. Set $N_c = Iround\left(\mu N \Delta t/(2\varepsilon)\right)$.
  7. Select $2N_c$ dummy collision pairs (i, j) uniformly among all possible pairs, and for those.
  8. Compute the relative cross section, σ_{ij}=$(\pi/4)\, d_{pq}^2 \left|v_i - v_j\right|$.
  9. Generate uniform random numbers (Rand).
  10. if $Rand < \sigma_{ij}/\bar{\sigma}$:
      (a) Perform the collision between i and j, and compute the post-collision velocities v_i^* and v_j^* according to the collisional law.
      (b) Generate two uniform random numbers ζ_1, ζ_2.
      (c) Set $\alpha = \cos^{-1}\left(2\xi_1 - 1\right), \beta = 2\pi\xi_2$.

(d) Set $\phi = (\cos\beta\sin\alpha \;\; \sin\beta\sin\alpha \;\; \cos\alpha)^T$.
(e) Set $v_i^* = \frac{1}{2}(v_i + v_j) + \frac{1}{2}|v_i - v_j|\,\phi$, $v_j^* = \frac{1}{2}(v_i + v_j) - \frac{1}{2}|v_i - v_j|\,\phi$.
(f) Set $v_i^{n+1} = v_i^*$, $v_j^{n+1} = v_j^*$.
else
(g) Set $v_i^{n+1} = v_i^n$, $v_j^{n+1} = v_j^n$.
(h) Set $v_i^{n+1} = v_i^n$ for the $N_i - 2N_c$ particles that have not been selected.

- End for
- Calculate macroscopic properties:
- macroscopic flow velocity: $\bar{v}_0 = \frac{1}{\rho}(m_p n_p \bar{v}_p + m_q n_q \bar{v}_q)$,
- density: $\rho = n.m$,
- thermal Velocity: $v_i' = \bar{v}_i - \bar{v}_0$.
- temperature: $T_{Tr} = \frac{1}{3kn}\left(n_p m_p v_p'^2 + n_q m_q v_q'^2\right)$.
- pressure: $P = nkT_{Tr} = \frac{1}{3}\left(n_p m_p v_p'^2 + n_q m_q v_q'^2\right)$.

During each step, all the other $N_i - 2N_c$ particle velocities remain unchanged. Here, by Iround(x), we denote a suitable integer rounding of a positive real number x. In our algorithm, we choose:

$$\text{Iround(x)} = \begin{cases} [x] & \text{with probability } [x] + 1 - x \\ [x] + 1 & \text{with probability } x - [x] \end{cases}$$

Algorithm of the Time Relaxed Monte Carlo Method (TRMC)

TRMC Algorithm.(first order TRMC scheme for the VHS collision model molecules).

- $T_{ref} = 273$ K
- $d_{p_{ref}} = 2.33 \times 10^{-10}$, for He
- $d_{q_{ref}} = 4.17 \times 10^{-10}$, for Ar
- $m_r = \frac{m_p m_q}{m_p + m_q}$
- $k = 1.380658 \times 10^{-23}$ jK^{-1}
- $\Delta t = 5 \times 10^{-6}$ Sec
- Distribute the initial locations of the particles according to the uniform distribution.
- Compute the initial velocity of the particles, $\{v_i^0, i = 1, ..., N\}$ by sampling them from the initial density f_0.
- for $n_t = 1$ to n_{tot}:
  1. Given $\{v_i^n, i = 1, \ldots, N\}$.
  2. Define the local Knudsen number (ε).
  3. Calculate

$$d_p = (d_{ref}) \left[\left\{2k\,(T_{ref}) \,/\, \left(m_r\,|v_i - v_j|^2\right)\right\}^{\gamma - 1/2} / \; \Gamma\,(5/2 - \gamma)\right].$$

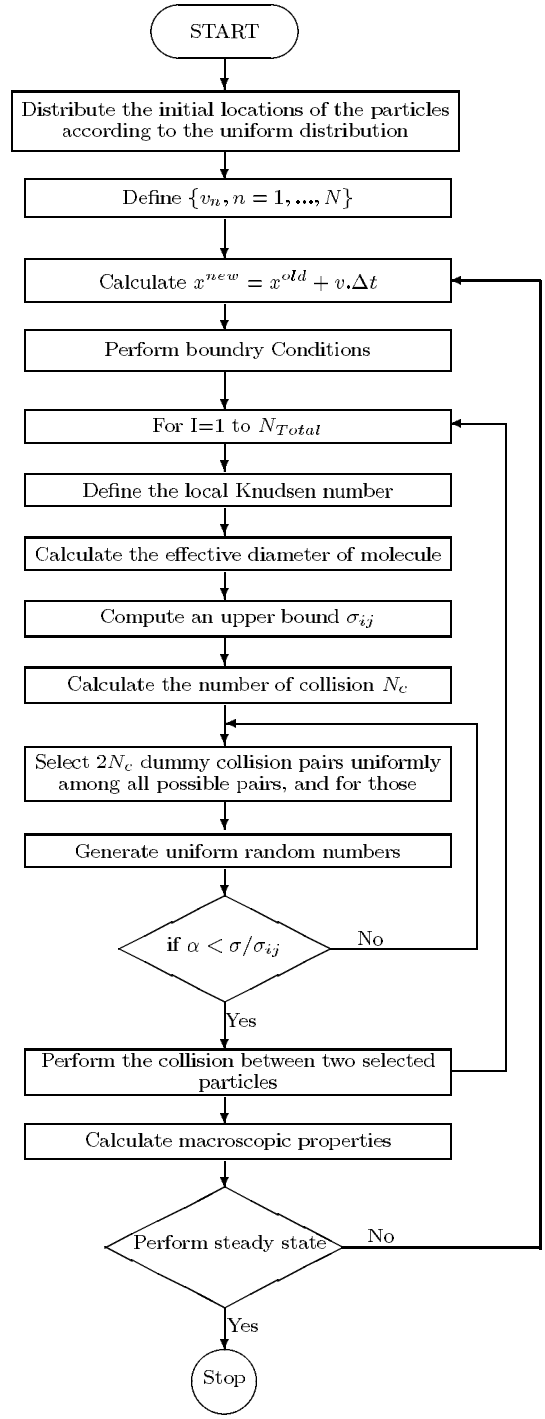

Figure 2. The Flowchart of DSMC Scheme.

4. Compute an upper bound $\bar{\sigma} = \max\left((\pi/4)\,d_p^2\,(|v_i - v_j|)\right)$ for the cross section, $\bar{\sigma}$ is updated in each collision.
5. Set $\tau = 1 - \exp\left(\rho\bar{\sigma}\Delta t/\varepsilon\right)$.
6. Compute $A_1(\tau) = \tau^2 - \tau^3$, $A_2(\tau) = \tau^3 - \tau^4$.
7. Set $N_c = \text{Iround}\,(NA_1/2)$.
8. Select N_c dummy collision pairs (i, j) uniformly among all possible pairs, and for those.
9. Compute the relative cross section, $\sigma_{ij} = (\pi/4)\,d_{pq}^2\,|v_i - v_j|$.

10. Generate uniform random numbers (Rand).
11. if $Rand < \sigma_{ij}/\bar{\sigma}$:
    (a) Perform the collision between i and j, and compute the post-collision velocities v_i^* and v_j^* according to the collisional law.
    (b) Generate two uniform random numbers ζ_1, ζ_2.
    (c) Set $\alpha = \cos^{-1}(2\xi_1 - 1), \beta = 2\pi\xi_2$.
    (d) Set $\phi = (\cos\beta\sin\alpha \;\; \sin\beta\sin\alpha \;\; \cos\alpha)^T$.
    (e) Set $v_i^* = \frac{1}{2}(v_i + v_j) + \frac{1}{2}|v_i - v_j|\phi$, $v_j^* = \frac{1}{2}(v_i + v_j) - \frac{1}{2}|v_i - v_j|\phi$.
    (f) Set $v_i^{n+1} = v_i^*$, $v_j^{n+1} = v_j^*$.
    else
    (g) Set $v_i^{n+1} = v_i^n$, $v_j^{n+1} = v_j^n$.
12. Set $N_M = \text{Iround}(NA_2)$
13. Select N_M particles among those that have not collided, and compute their mean momentum and energy.
14. Sample N_M particles from the Maxwellian with the above momentum and energy, and replace the N_M selected particles with the sampled ones.
15. Set $v_i^{n+1} = v_i^n$ for all the $N - 2N_c - N_M$ particles that have not been selected.

- End for
- Calculate macroscopic properties:
- macroscopic flow velocity: $\bar{v}_0 = \frac{1}{\rho}(m_p n_p \bar{v}_p + m_q n_q \bar{v}_q)$,
- density: $\rho = n.m$,
- thermal Velocity: $v_i' = \bar{v}_i - \bar{v}_0$.
- temperature: $T_{Tr} = \frac{1}{3kn}\left(n_p m_p v_p'^2 + n_q m_q v_q'^2\right)$.
- pressure: $P = nkT_{Tr} = \frac{1}{3}\left(n_p m_p v_p'^2 + n_q m_q v_q'^2\right)$.

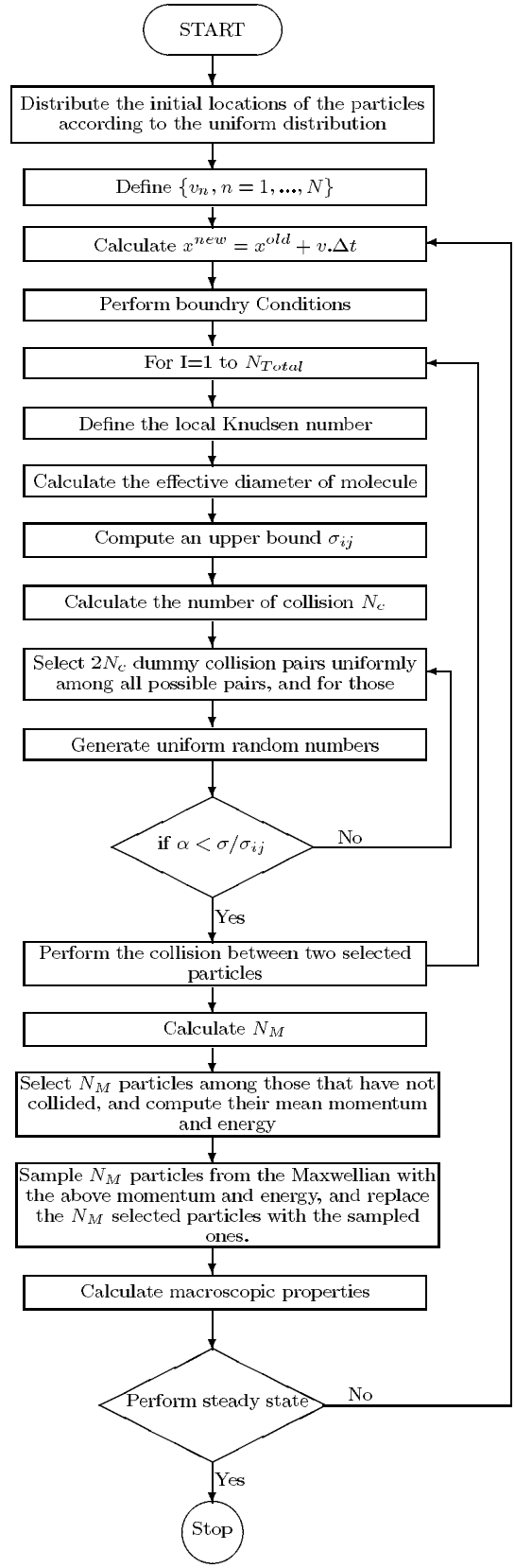

Figure 3. The Flowchart of DSMC Scheme.

THE NUMBER OF MODEL MOLECULES DEPENDENCY TEST

The number of model molecules dependency test is done using more model molecules in each mesh. The simulation is done using 35700 model molecules in the grid system; however, in the number of model molecules dependency test the number of model molecules is increased to 57120 model molecules in our grid system. The results of simulation of flow characteristics for the two cases (35700 model molecules and 57120 model molecules in the grid system) at 4 seconds of real time of flow simulation are obtained and compared with each other. Figure 4, Figure 5, Figure 6, and Figure 7 show the number of molecules dependency test for density, number density, temperature and swirl velocity respectively. Figure 4 shows the number of model molecules dependency test for the mixture density. The maximum discrepancy between the results of simulation of number of model molecules dependency test for

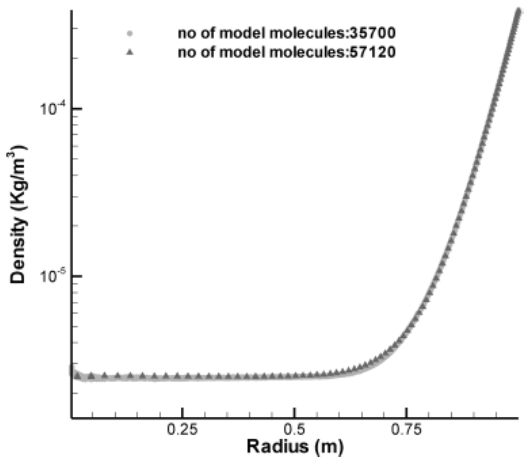

Figure 4. The number of molecules dependency test for density.

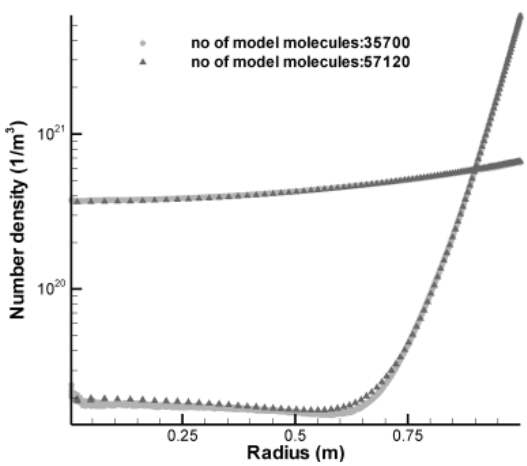

Figure 5. The number of molecules dependency test for number density.

the mixture density for the two cases (35700 model molecules and 57120 model molecules in the grid system) is less than 4% at 0.625 meter of radial distance inside the cylinder. Figure 5 shows the number of model molecules dependency test for number densities of argon and helium. The maximum discrepancy between the results of simulation of number of model molecules dependency test for the number density of argon and helium for the two cases (35700 model molecules and 57120 model molecules in the grid system) are less than 7.3% at 0.625 meter of radial distance inside the cylinder and less than 1.35% at 0.1 meter of the radial distance inside the cylinder respectively. Figure 6 shows the number of model molecules dependency test for the temperature. The maximum discrepancy between the results of simulation of number of model molecules dependency test for the temperature for the two cases (35700 model molecules and 57120 model molecules in the grid system) is less than 0.66% at 0.75 meter of radial distance inside the cylinder. Figure 7 shows the number of model molecules dependency test for the swirl velocity. The maximum discrepancy between the results of simulation of number of model molecules dependency test for the swirl velocity for the two cases (35700 model molecules and 57120 model molecules in the grid system) is less than 4.37% at 0.625 meter of radial distance inside the cylinder.

THE RESONANCE CONDITION TEST

The resonance condition is studied for the rotating cylinder. The natural frequencies of the rotating cylinder are determined. Here are the results of simulation for the modal natural frequencies using the ANSYS software shown in Table 1 below. For the sake of simplicity, we just assume a three degree of freedom model in our simulation. The matrix form the three degree of freedom equation of the rotating cylinder is as follows:

$$M\ddot{X} + KX = 0 \tag{33}$$

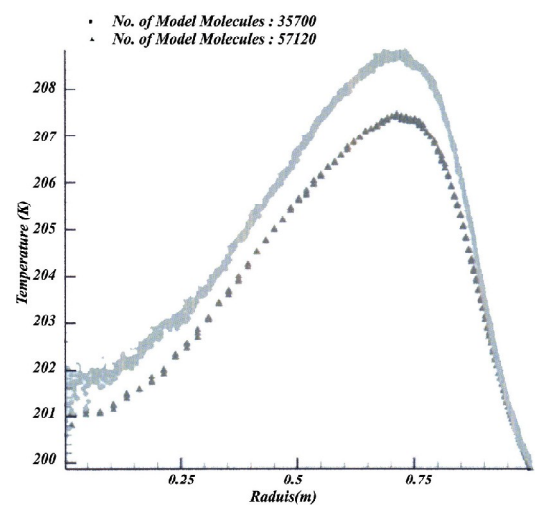

Figure 6. The number of molecules dependency test for Temperature.

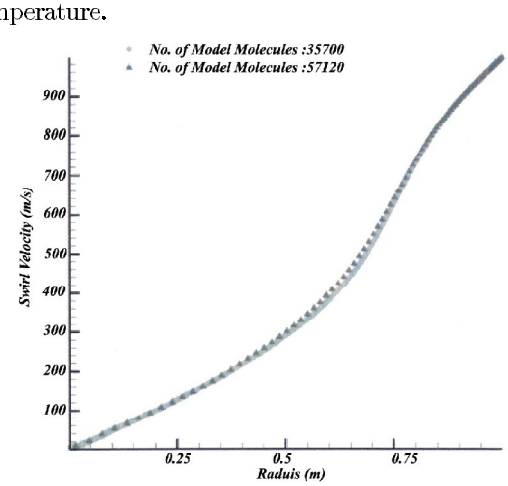

Figure 7. The number of molecules dependency test for Swirl Velocity.

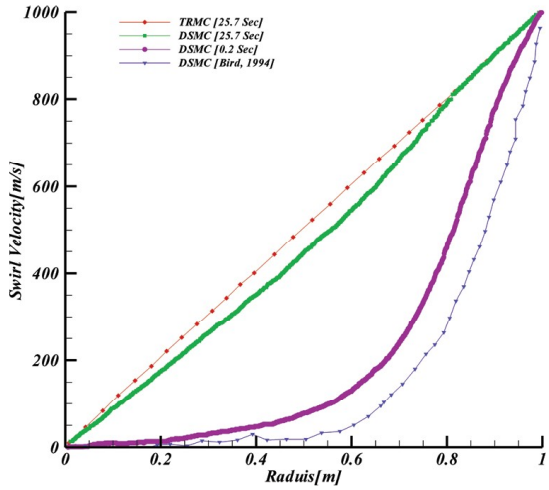

Figure 8. Comparison between the results of simulation using the DSMC method, the TRMC scheme and the results of Bird, 1994 for the variations of the swirl velocity along the radial coordinates.

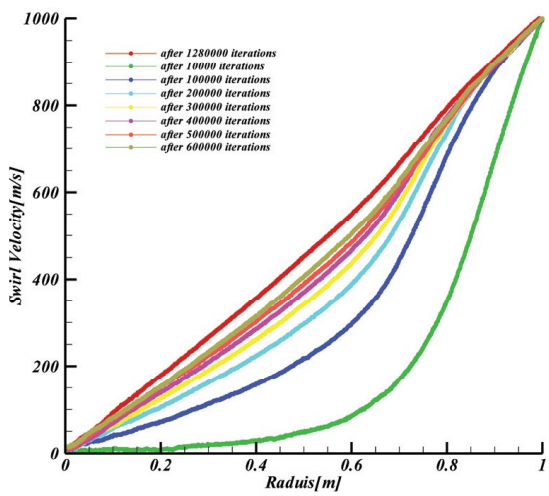

Figure 9. Comparison between the results of simulation using the DSMC method, the TRMC scheme and the results of Bird, 1994 for the variations of the swirl velocity along the radial coordinates and the time evolution of the variations of swirl velocity along the radial coordinates from the 0.2 second of real time (10000 iterations) up to 25.7 seconds of real time (1280000 iterations) respectively.

where

$$M = \begin{bmatrix} \left(\frac{m}{2} + \frac{2I}{l^2}\right) & \left(\frac{m}{4} - \frac{I}{l^2}\right) & 0 \\ \left(\frac{m}{4} - \frac{I}{l^2}\right) & \left(\frac{m}{2} + \frac{2I}{l^2}\right) & \left(\frac{m}{4} - \frac{I}{l^2}\right) \\ 0 & \left(\frac{m}{4} - \frac{I}{l^2}\right) & \left(\frac{m}{2} + \frac{2I}{l^2}\right) \end{bmatrix} \tag{34}$$

$$k = \frac{K}{l^2} \begin{bmatrix} 5 & -4 & 1 \\ -4 & 6 & -4 \\ 1 & -4 & 5 \end{bmatrix} \tag{35}$$

and

$$K = 1140 \frac{N.m}{rad}$$

$$l = 1\,m$$

$$m = 0.971\,Kg$$

$$I = 1.21714 \times 10^{-2}\,Kg.m^2 \tag{36}$$

DISCUSSION

Figure 10 shows the comparison of the results of simulations using the DSMC method and the TRMC scheme with the results of Bird, 1994 for the variations of the swirl velocity along the radial coordinates. Comparison of our results of simulation using the DSMC method for the swirl velocity with the results of Bird, 1994 shows good agreement at 0.2 second of real time (10000 iterations); however, comparisons of our results of simulations using the DSMC method at 25.7 seconds of real time (1280000 iterations) and the results of simulation using the TRMC scheme at 25.7 seconds of real time (256000 iterations) with the results of Bird, 1994 show high discrepancies. The discrepancies are due to the lack of sufficient real time (number of iterations) in the calculation of Bird, 1994 simulation. In the Bird, 1994 simulation the DSMC method is used; however, the larger time-steps are not allowed (Pareschi, et al, 2005); therefore, one is not able to reach the stationary flow simulation. Comparisons of our results of simulation using the DSMC method at 25.7 seconds of real time (1280000 iterations) for the swirl velocity with the results of simulation using the

Table 1. Shows the modal natural frequencies of the rotor with three degree of freedom without and with rotational speed.

Mode of Natural Frequency	Natural Frequency[Hz] without Rotation	Natural Frequency[Hz] with Rotation(60000.rpm)
1	115	140
2	272	476
3	309	976
4	426	1000
5	442	1367
6	633	1375
7	760	1392
8	765	1407
9	782	1487
10	820	1598
11	889	1632
12	911	1851
13	931	2139
14	952	2179
15	995	2268
16	-	2484
17	-	2639
18	-	2641

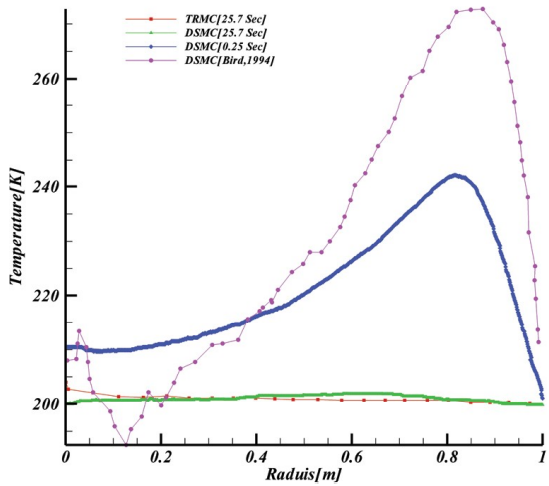

Figure 10. Comparison between the results of simulation using the DSMC method, the TRMC scheme and the results of Bird, 1994 for the variations of the temperature along the radial coordinates.

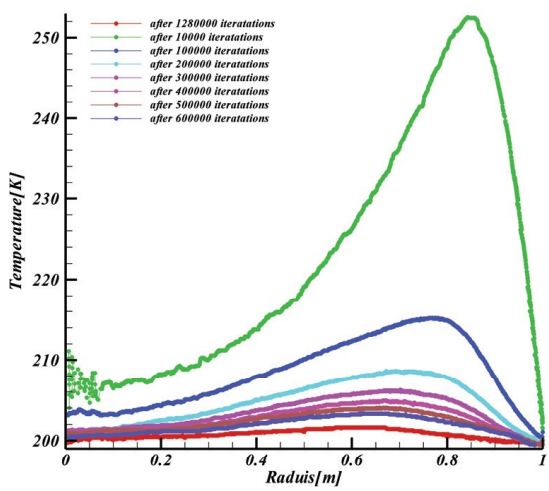

Figure 11. Comparison between the results of simulation using the DSMC method, the TRMC scheme and the results of Bird, 1994 for the variations of the temperature along the radial coordinates and the time evolution of the variations of temperature along the radial coordinates from the 0.25 second of real time (12500 iterations) up to 25.7 seconds of real time (1280000 iterations).

TRMC scheme at 25.7 seconds of real time (256000 iterations) show good agreements. Figure 9 shows the time evolution of the variations of swirl velocity along the radial coordinates for different iterations (10000 to 1280000 iterations). Figure 10 shows a comparison of the results of simulations using the DSMC method and the TRMC scheme with the results of Bird, 1994 in the variations of the gas mixture (argon and helium) temperature along the radial coordinates. Comparison of the results of simulation using the DSMC method for the gas mixture (argon and helium) temperature with the results of Bird 1994 shows good agreements at 0.2 second of real time (10000 iterations); however, comparisons of our results of simulations using the DSMC method at 25.7 seconds of real time (1280000 iterations) and the results of simulation using the TRMC scheme at 25.7 seconds of real time (256000 iterations) with the results of Bird, 1994 show high discrepancies. The discrepancies are due to lack of sufficient real time computing (number of iterations) in the Bird, 1994 calculations. Although in those calculations where the DSMC method is used one is unable to choose larger time steps, in the simulation using the TRMC scheme one is allowed to choose larger time-steps (see Pareschi et al, 2005); therefore, reaching larger real time for calculations. Comparisons of our results of simulation using the DSMC method at 25.7 seconds of real time (1280000 iterations) for the gas mixture (argon and helium) temperature with the results of simulation using the TRMC scheme at 25.7 seconds of real time (256000 iterations) show good agreements. Figure 11 shows the time evolution of the variations of the gas mixture (argon and helium) temperature along the radial coordinates for different iterations (10000 to 1280000 iterations). Figure 12 shows the comparison of the results of simulations using the DSMC method with the TRMC scheme for the variations of the gas mixture (argon and helium) pressure along the radial coordinates. Figure 12 shows that at 25.7 seconds of real time (1280000 iterations) the values of pressure around the wall of the cylinder are approximately 18 times bigger than the values of pressure around the center of the cylinder.

Comparisons of Number Density Results with the Analytical Solution

The analytical solution of Kuo (1990) is only used here as a reference to render comparison of the results of the present simulation. The solution of Kuo (1990) is based on the assumption that the flow is in equilibrium. Here in the present simulation one assumes that the results of our simulation reach the equilibrium condition as well. However, this assumption is not completely valid. Therefore, the analytical solution of Kuo (1990) can only be used as a reference and not as an absolute source to judge the accuracy of the TRMC scheme.

Figure 13, 14 and 15 show the comparisons of the DSMC method, the TRMC scheme and the results of Bird, 1994 with the analytical solution for the variations of the density of gas mixture, the number density of helium and the number density of argon along the radial coordinate respectively. Comparison of our results of simulation for the density of gas mixture (Figure 13) with the analytical solution shows reasonable agreement and the agreement is pronounced for the radial distance of $r > 0.5\,\mathrm{m}$; however, the comparison of our results of simulation using the DSMC and the TRMC with the analytical solution shows better agreement than the results of Bird, 1994 (Figure 13). Comparison of our results of simulation

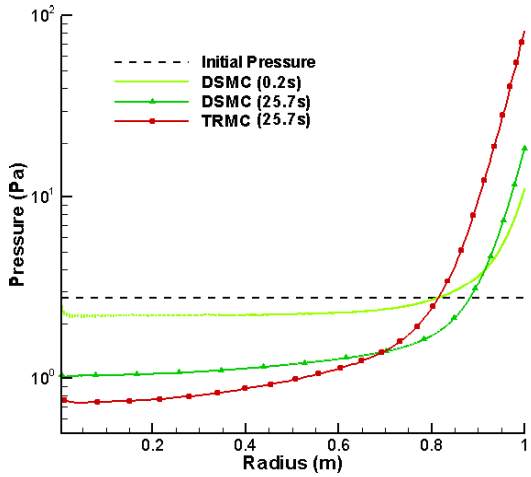

Figure 12. Comparison between the results of simulations using the DSMC method, the TRMC scheme for the variations of the gas mixture (argon and helium) pressure along the radial coordinates.

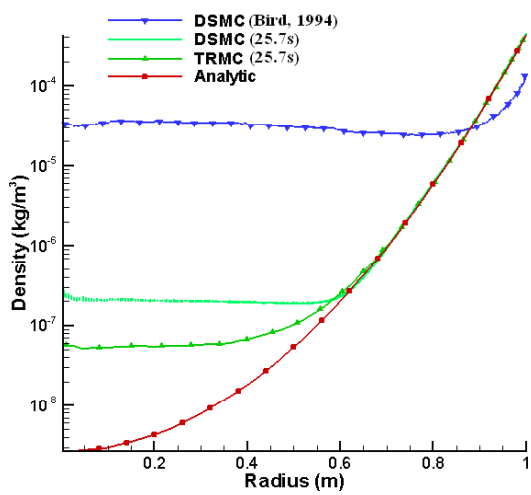

Figure 13. Comparison between the DSMC scheme, the TRMC scheme and the results of Bird 1994 with the analytical solution for the variations of the number density of helium.

for the number density of helium (Figure 14) with the analytical solution shows a reasonable agreement, which is pronounced for the radial distance of $r > 0.5$ m; however, comparison of the results of simulation of Bird, 1994 in the number density of helium (Figure 14) with the analytical solution shows high discrepancies. The discrepancies of Bird, 1994 results are due to the lack of sufficient real time in the simulation using the DSMC method. In the simulation using the DSMC method, one is not allowed to choose larger time-steps; therefore, reaching the larger real time is very difficult. However, in the simulation using the TRMC scheme, one is allowed to choose larger time-steps in order to reach larger real time. Comparison of our results of simulation in the number density of argon (Figure 15) with the analytical solution shows better agreement than its counterpent in Bird, 1994.

CONCLUSION

The comparison of the results of simulation using the DSMC method with the results of the simulation using the TRMC scheme for the swirl velocity and the temperature shows good agreement. However, similar comparisons of Bird 1994 with the analytical solution demonstrates high discrepancies. The comparisons of the results of simulations using the DSMC method and the TRMC scheme with the analytical solution for the density, number density of helium and number density of argon also show good agreement. However, again the same comparisons using Bird 1994 show high discrepancies. The conclusions are summarized as follows:

1. Due to the required small time-steps in the DSMC simulations, the discrepancies of the results using the DSMC method is pronounced in comparison with the results of the simulations using the TRMC scheme.

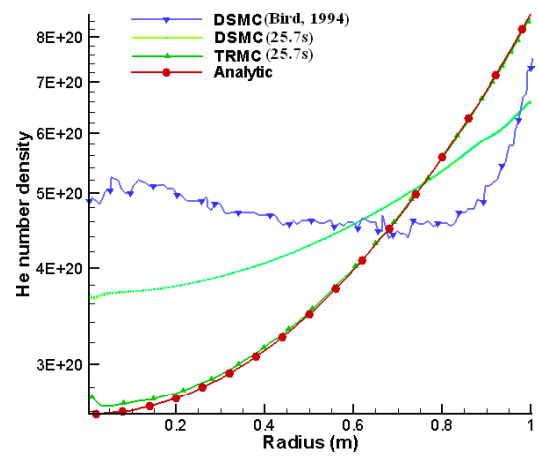

Figure 14. Comparison between the DSMC scheme, the TRMC scheme and the results of Bird 1994 with the analytical solution for the variations of the number density of argon.

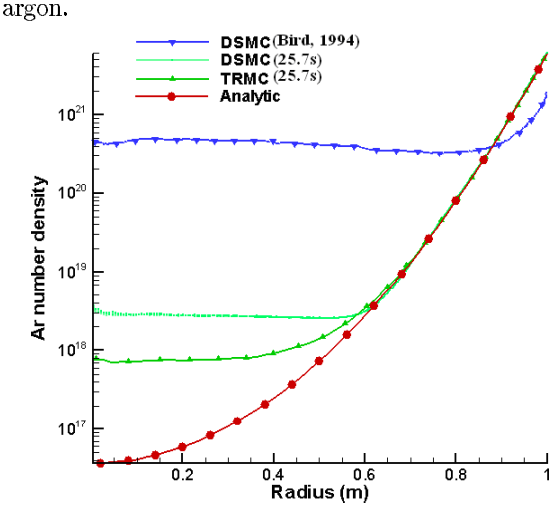

Figure 15. Comparison between the DSMC scheme, the TRMC scheme and the results of Bird 1994 with the analytical solution for the variations of the density.

2. The comparisons of the results of simulations using the TRMC scheme for the density and the number density with the analytical solution show better agreement than those obtained through DSMC method.
3. Having larger time-steps in the simulation using the TRMC scheme allows one to reach stationary results for the flow characteristics in shorter time; therefore, the results of the simulations using the TRMC scheme show improvements over similar results using the DSMC method. In our simulation, there are two sources of approximation errors. First, the approximation errors inherent in the selection of larger time-step used in the TRMC scheme. Second, the approximation errors due to modeling the molecular collision, the VHS model, used in the present work. These two sources of approximation errors interact with each other. The nature of the interaction of the two sources of approximation errors is very complicated. However, the results of our simulation in the present work show that the approximation errors inherent in the selection of larger time-steps in the TRMC scheme counteract with the other sources of approximation errors inherent in the simulation modeling such as modeling of molecular collisions, *i.e.* the VHS model, used in the present work. Therefore, the results of the simulation using the TRMC scheme show improvement over the results of simulation using the DSMC method.

REFERENCES

1. Babovsky H., "On a Simulation Scheme for the Boltzmann Equation", *Mathematical Method in the Applied Sciences*, **8**, PP 223-233(1986).
2. Bird G. A., *Molecular Gas Dynamics and the Direct Simulation of Gas Flows*, Oxford Univ. Press, (1994).
3. Bottoni M., "Molecular Approach to Sodium Vapor Condensation, Rewetting and Vaporization in LMFBR Bundle under Hypothetical Accident Conditions", *J. Nuclear Science and Technology*, **41**(5), PP 579-593(2004).
4. Cercignani C., "The Boltzmann Equation and Its Applications, Lectures Series in Mathematics", *Springer-Verlag*, Berlin, New York, **68**, (1988).
5. Crifo J.E., Lukianov G.A., Rodionov A.V., Khanlarov G.O. and Zakharov V.V., "Comparison Between Navier-Stokes and Direct Monte-Carlo Simulation of the Circumnuclear Coma", *Icarus*, **156**, PP 249-268(2002).
6. Gabetta E., Pareschi L. and Toscani G., "Relaxation Schemes for Nonlinear Kinetic Equations", *SIAM J. Number. Anal.*, **34**, PP 2168-2194(1997).
7. Hockney R. W. and Eastwood J. W., *Computer Simulation Using Particles*, Mc-Graw Hil International Book Co., (1981).
8. Kuo L. Y., *Problems and Solutions on Thermodynamics and Statistical Mechanics*, World Scientific Publication, (1990).
9. Longair M. S., *Theoretical Concepts in Physics, An Alternative View of Theoretical Reasoning in Physics*, Cambridge University Press., (2003).
10. Moss J. N., Bird G. A., "Direct Simulation of Transitional Flow for Hypersonic Reentry Conditions", *Progress in Astronautics and Aeronautics*, **96**, PP 113-139(1985).
11. Myong R. S., "A generalized Hydrodynamic Computational Model for Rarified and Micro Scale Gas Flows", *Journal of Computational Physics*, **195**, PP 655-676(2004).
12. Nanbu K., "Direct Simulation Scheme Derived From the Boltzmann Equation", *Journal of the Physical Society of Japan*, **49**, PP 2042-2049(1980).
13. Nanbu K., "Theoretical Basis of the Direct Simulation Monte Carlo Method", *Proceeding of the 15th International Symposium on Rarefied Gas Dynamics*, PP 369-383.
14. Nourazar S.S., Hosseini S.M., Ramezani A. and Dehghanpour H.R., "Comparison Between the Navier-Stokes and the Boltzmann Equations for the Simulation of an Axially Symmetric Compressible Flow with Shock Wave Using the Monte-Carlo Method", *Computational Methods and Experimental Measurements XII, WIT Transaction on Modeling and Simulation*, **41**, PP 61-69(2005).
15. Pareschi L., Calfisch R. E., "An Implicit Monte-Carlo Method for Rarefied Gas Dynamics", *J. Comput. Phys.*, **154**(90), (1999).
16. Pareschi L., Russo G., "Time Relaxed Monte-Carlo Methods for the Boltzmann Equation", *SIAM J. Sci. Comput.*, **23**, PP 1253-1273(2001).
17. Pareschi L., Trazzi S., "Asymptotic Preserving Monte Carlo Methods for the Boltzmann Equation", *Transport Theory Statist. Phys.*, **29**, PP 415-430(2005).
18. Pareschi L., Trazzi S., "Numerical Solution of the Boltzmann Equation by Time Relaxed Monte-Carlo (TRMC) Method", *International Journal of Numerical Method in Fluids*, **48**, PP 947-983(2005).
19. Shinagawa H., Setyawan H., Asai T., Sugiyama Y. and Okuyama K., "An Experimental and Theoretical Investigation of Rarified Gas Flow Through Circular Tube of Finite Length", *Pergamon, Chemical Engineering Science*, **56**, PP 4027-4036(2002).
20. Wild E., "On Boltzmann's Equation in the Kinetic Theory of Gases", *Proc. Camb. Phil. Soc.*, **47**, PP 602-609(1951).